PACS: 41.60.-m; 61.80.Cb, 61.85.+p, 41.50.+h

DIFFRACTION, EXTRACTION AND FOCUSING OF PARAMETRIC X-RAY RADIATION, CHANNELING RADIATION AND CRYSTAL UNDULATOR RADIATION

A.V. Shchagin
National Science Center Kharkov Institute of Physics and Technology, Kharkov 61108, Ukraine
E-mail: shchagin@kipt.kharkov.ua
Received August 6, 2006

The paper describes the possibility of producing a focused parametric X-ray radiation (PXR) without applying any special X-ray optics. The PXR is emitted by relativistic charged particles that are channeling along a bent crystal. The PXR emitted from the whole length of the bent crystal is brought into focus. Some properties of focused PXR are estimated for typical experimental conditions, its possible applications are discussed. Besides, the feasibility of diffraction of parametric X-ray radiation emitted by relativistic particles in a bent crystal is described for the first time. The PXR generated at one set of crystallographic planes may be diffracted by another set of crystallographic planes in the same bent crystal. In the example being, the PXR is emitted in the backward direction and undergoes diffraction at a right angle. After diffraction, the PXR escapes from the thin crystal and becomes focused. Some properties of the diffracted focused PXR are estimated for typical experimental conditions. The experiment for observation of focused non-diffracted and diffracted PXR is proposed. Application of focused PXR for online control of the bent crystal and paricle beam state and the bent crystal alignment is proposed. Besides, possibilities for diffraction, extraction and focusing of crystal undulator radiation, as well as focusing of channeling radiation from a bent crystal are proposed. The installation of X-ray detector(s) in the vicinity of Bragg direction(s) is proposed in forthcoming experiments with crystalline undulator for observation of undulator radiation and online control of the undulator and particle beam state and also undulator alignment.
KEY WORDS: parametric X-ray radiation, channeling radiation, crystal undulator radiation, diffraction of X-rays, bent crystal, channeling particles, focusing of X-rays, virtual images, focusing of channeling radiation, focusing of crystal undulator radiation.

The possibility of steering charged particle motion by a bent crystal has first been predicted by Tsyganov [1]. The steering can be realized for the particles which are traveling through a long bent crystal in the channeling regime [2]. The channeling particles may be deflected, if the crystal is bent smoothly enough. Experiments on proton beam deflection, focusing and extraction by bent crystals have been performed, e.g., in Gatchina [3] at proton beam energy 1 GeV, Serpukhov at 70 GeV [4,5], CERN at 120 GeV [6] and at 450 GeV [7,8], Fermilab at 900 GeV [9]. The steering of positive particles at planar channeling is most effective (see, e.g., [7]). Bent crystals of about several centimeters in length are generally used in the experiments. The crystals seem to be convenient for production, diffraction, extraction and focusing of parametric X-ray radiation (PXR), channeling radiation (ChR) and crystal undulator radiation (CUR) generated by channeling relativistic particles.

The first theoretical predictions of the PXR one can find e.g. in [10-12]. Experimental studies on the PXR from relativistic electrons moving through a thin crystal have been performed since 1985 to gain an insight into the PXR properties and to develop a new source of a quasimonochromatic polarized X-ray beam. The PXR has its maximum intensity in the vicinity of the Bragg direction relative to the crystallographic plane (PXR reflection). The PXR reflection from crystals was observed and investigated at electron beam energies ranging from a few MeV to several GeV, and at PXR energies from a few keV to hundreds of keV. The validity of kinematic theory [11] for the description of PXR properties has been demonstrated in the most of related publications. General information about the nature, properties and investigations of the PXR, as well as references to original papers can be found, e.g., in reviews [13-16]. The experiments on observation of PXR from protons has been described in [17,34]. The idea about generation of focused PXR from a bent crystal has been proposed in [18,28].

In the present paper we will describe the possibility of focusing the PXR generated in a bent crystal by channeling particles and consider some of its properties. Besides, the consideration will be given to the diffraction and focusing of PXR emitted in the backward direction in bent crystal. The experiment will be proposed for observation of focused (both non-diffracted and diffracted) PXR. In the end, we will briefly discuss the possibilities for extraction and focusing of CUR and ChR generated by channeling positrons in a crystal.

HOW TO FOCUS THE PXR

Let us suppose that relativistic charged particles are moving along a bent crystalline plate in the channeling regime, as it is shown in Fig. 1. The bent crystal is cylindrical in shape, R being the radius, and f is the axis of the cylinder. The particles are channeling along the crystallographic planes denoted by the reciprocal lattice vector $\vec{g}$. We will consider the PXR reflections from crystallographic planes aligned at 45° relative to the particle trajectory and perpendicular to the plane of Fig. 1a. These crystallographic planes are denoted by the reciprocal lattice vectors $\vec{g}_1$ and $\vec{g}_2$. The PXR reflections from the planes are going perpendicularly to the particle trajectory and the crystalline plate

surface. The PXR reflections from $\vec{g}_1$ are going from the whole plate to the axis f, or, in other words, the PXR reflections are focused. The PXR reflections from $\vec{g}_2$ are going in opposite directions, i.e., from the axis f. Thus, the PXR generated on the crystallographic planes $\vec{g}_1$ in the whole bent crystal will be collected (focused) on the axis f.

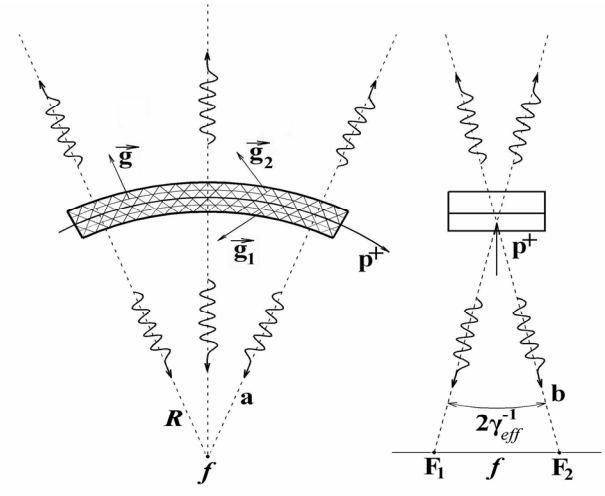

Fig. 1. Production of focused PXR by particles channeling in a bent crystalline plate.
Side and front views are shown at the left (a) and right (b) respectively. The particle beam is indicated by arrows p^+. The particles are channeling along the crystallographic planes denoted by the reciprocal lattice vector $\vec{g}$. The single-crystal plate is cylindrical in shape with a radius of curvature R around the axis f. The wavy lines with arrows show the direction of radiation propagation at the maxima of the PXR reflections. The PXR reflections from the crystallographic planes denoted by the reciprocal lattice vector $\vec{g}_1$ are focused at points F_1 and F_2 on the axis f. The PXR reflections from the crystallographic planes denoted by the reciprocal lattice vector $\vec{g}_2$ are going in opposite directions and form virtual images of points F_1 and F_2. The PXR focused at points F_1 and F_2 is linearly polarized practically in the plane of Fig. 1b.

The Huygens-Fresnel construction for formation of the PXR from a perfect crystal may be found in [14,16]. Here, Fig. 2 shows the Huygens-Fresnel construction for formation and focusing of the PXR wavetrain from a bent crystal. The spherical wavefronts are going from the points, where the particle crosses the crystallographic planes denoted by the reciprocal lattice vector $\vec{g}_1$. They are going to the focuses with a phase difference divisible by 2π and form the PXR wavetrain. For brevity, here we call such formation as the PXR focusing. Evidently, that the PXR energy (frequency) in the radial direction is the same as the energy (frequency) for the PXR at a right angle to the particle beam, $E = \hbar\omega = \frac{V\hbar g_1}{\sqrt{2}}$.

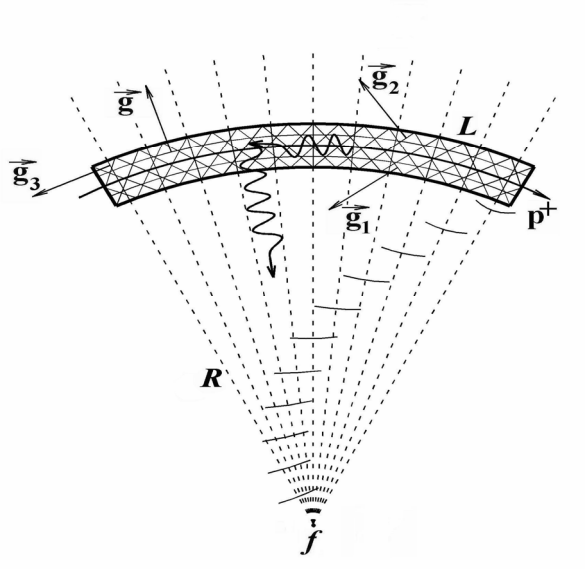

Fig. 2. The Huygens-Fresnel construction for focusing of the PXR wave train.

Spherical surfaces of equal phase (spherical wave fronts) are going from the points, where the channeling particle crosses the crystallographic planes $\vec{g}_1$. Parts of spherical wavefronts are shown on the radial lines R at the moment, when the particle is at the end of the right arrow p^+. The wave train of length $l = \frac{cL}{V}$ with the wave length $\lambda = \frac{c2\pi\sqrt{2}}{Vg_1}$ and the number of periods $n = \frac{Lg_1}{2\pi\sqrt{2}}$ is focused in the vicinity of axis f. Besides, the backward-going PXR is generated on the crystallographic planes denoted by the reciprocal lattice vector $\vec{g}_3$. It is shown by a horizontal wavy line with the arrow. Then it is diffracted on the crystallographic planes denoted by the reciprocal lattice vector $\vec{g}_2$ and is focused at the axis f.

From the classical point of view, the train of PXR waves arrives at the focus. The direction of train propagation changes within the small angle $\frac{L}{R}$. The relative natural PXR spectral peak width may be estimated as $\left(\frac{\Delta E}{E}\right)_{nat} \sim \frac{1}{n}$, where n is a number of crystallographic planes crossed by the particle, that is equal to the number of wavelengths in the train.

From the quantum point of view, the PXR quantum can arrive at the focus on the axis f for the time $\Delta t = \frac{L}{V}$ of the particle motion through the crystal. In this case, the PXR spectral peak width may be estimated from the Heisenberg principle $\Delta E \Delta t \sim \hbar$. With the use of the expression for the PXR frequency, this principle gives $\frac{\Delta E}{E} \sim \frac{1}{2\pi n}$. Thus, the classical and quantum approaches give practically the same, very narrow relative natural spectral peak width of about $\frac{1}{n}$. However, in a real experiment, the broadening of the PXR spectral peak width should be due to a limited angular resolution of the both detector and the whole experiment, to a non-ideal cylindrical shape of the crystal, radiation of non-channeling particles and other experimental factors.

The properties of the PXR reflection generated at a right angle to the particle beam in thin crystals have been studied in several papers. The image of the whole PXR reflection at a right angle to the particle beam was first observed in [19], its polarization was considered in [20], and a detailed structure of the angular distribution of yield was studied in [21]. The shape of the angular distribution of the yield may be found, e.g., in figures of [19, 21, 16]. The shape of angular distribution of linear polarization directions in the PXR reflection at the right angle to the particle trajectory may be found, e.g., in figures of [20, 16].

The angular distribution of the PXR yield in the reflection at a right angle to the particle trajectory has two maxima in the plane of Fig. 1b. Therefore the PXR will be focused at two points F_1 and F_2 in the axis f at an angular distance of about $2\gamma_{eff}^{-1}$ one from another. Here, γ_{eff} is the effective relativistic factor in the medium [16] with the Ter-Mikaelian density effect taken into account, $\gamma_{eff}^{-1} = \sqrt{\gamma^{-2} + |\chi_0|}$, where γ is the relativistic factor of incident particles, χ_0 is the dielectric susceptibility of the medium. The PXR is linearly polarized in the vicinity of points F_1 and F_2. The linear polarization direction is practically in the plane of Fig. 1b. Thus, the focused PXR is linearly polarized in the plane of Fig. 1b. The size of the PXR spots focused around the points F_1 and F_2, is about $\sim \gamma_{eff}^{-1} R$. The PXR energy (frequency) in the vicinity of points F_1 and F_2 varies as $\Delta E = E\frac{b}{R}$ with a shift of the observation point at a distance b from the axis f in the horizontal direction, and remains unchanged at shifts of the observation point along the f axis [11, 16, 21].

Apart from the PXR emission, the particles moving through the crystalline plate ionize the crystal atoms, and thus make them emit the characteristic X-ray radiation (CXR). The CXR is isotropic and not focused, but it exists at points F_1 and F_2, too.

Further, the backward-going PXR should be focused at the same points F_1 and F_2. This radiation is generated by channeling particles at the crystallographic planes denoted by the reciprocal lattice vector $\vec{g}_3$ in Fig. 2. It propagates in the vicinity of the angle 180° to the particle trajectory and is shown by a horizontal wavy line with the arrow in Fig. 2. At a certain path length, the PXR frequency will satisfy the Bragg condition for the crystallographic planes $\vec{g}_2$. Therefore, a part of the backward-going PXR polarized in the plane of Fig. 1b will undergo the Bragg diffraction. The direction of propagation of diffracted PXR is shown by a wavy line with the arrow along the radius R of the crystal

curvature in Fig. 2. Thus, a part of backward PXR will be focused in the vicinity of the same points F_1 and F_2. The energy, the linear polarization and the spot size of diffracted backward PXR focused around the points F_1 and F_2 are practically the same as in the case of non-diffracted PXR.

ESTIMATION OF SOME PROPERTIES OF FOCUSED PXR

To understand the main features of focused PXR, let us estimate them for typical experimental conditions. As an example, we have performed calculations for 70 and 450 GeV protons channeling along the crystallographic plane (110) with the reciprocal lattice vector $\vec{g} =< \bar{1}\,\bar{1}0 >$ (see Fig. 1) in the Si single-crystal plate, 0.5 mm in thickness and $L = 5$ cm in length, with the radius of curvature $R = 5$ m. The PXR reflections under consideration are generated at the crystallographic planes parallel to the ones denoted by the reciprocal lattice vectors $\vec{g}_1 =< 100 >$ and $\vec{g}_2 =< 0\,\bar{1}0 >$. The calculations were performed using formulae from [14, 16, 24], derived within the framework of the Ter-Mikaelian theory [11]. The focused PXR reflections arrive at the points F_1 and F_2 from the crystallographic planes having a nonzero structure factor parallel to (100), these are the (400), (800), (12 00) planes. The PXR reflections from higher-index planes have substantially lower yields. The PXR reflections from similar crystallographic planes, that are parallel to $(0\,\bar{1}0)$, are going in opposite directions from the axis f. They form virtual images of focal points F_1 and F_2.

The $< \bar{1}10 >$ axis is aligned along the proton beam in the above-considered example. To avoid axial channeling in the experiment, one has to provide misorientation of the crystal lattice in the (110) plane for a small angle, which is somewhat larger than the critical channeling angle. The critical channeling angle for the Si single crystal at proton energies of 70 and 450 GeV is about $2.4 \cdot 10^{-5}$ and $1 \cdot 10^{-5}$ radian, respectively [2]. The main features of PXR emission, the positions of points F_1, F_2, and the properties of focused PXR will change only slightly at such a small misorientation.

The PXR properties are functions of the relativistic factor of the incident particle and the absolute value of particle charge [11, 14, 24]. Therefore, the results of present calculations might be valid for 38 and 245 MeV positrons and electrons, which have the same relativistic factors. However, the motion of these particles in a long crystal can differ from the motion of protons. For example, a significant part of high-energy protons can move through a long bent crystal in the channeling regime [2-9]. But electrons strongly scatter at channeling. So far as we know, there have been no publications about experimental research on channeling of positrons in bent crystals and on generation of PXR by positrons in any crystals.

ESTIMATION OF SOME PROPERTIES OF CXR

The yield of CXR at 1.74 keV due to K-shell ionization of Si atoms by 70 and 450 GeV protons was estimated in accordance with the recommendations from [26]. In the calculations, the K-shell ionization cross section for Si atoms was taken to be 1654 and 1946 barn. These cross section values were calculated for 38 and 245 MeV electrons having the relativistic factor identical to that of 70 and 450 GeV protons. The effect of channeling was not taken into account in the present estimation of the CXR yield, as it is not expected to be very significant at high particle energies (see [26]).

All calculations were performed for a uniform distribution of protons in the crystalline plate thickness. The radiation excited by channeling protons is going to the points F_1 and F_2 across the plate, and is attenuated by the Si crystal. The attenuation of PXR and CXR in the plate was taken into account in the calculations.

ESTIMATION OF SOME PROPERTIES OF BACKWARD-GOING DFFRACTED FOCUSED PXR

Particles generate the backward-going PXR at the crystallographic planes with non-zero structure factors $(4\bar{4}0),(8\bar{8}0),(12\,\bar{12}\,0)$ that are perpendicular to the particle trajectory and parallel to the ones denoted by the reciprocal lattice vector $\vec{g}_3$ in Fig. 2. The maximum yield in the PXR reflection is at the angle $\pi - \gamma_{eff}^{-1}$ relative to the tangent to the particle trajectory. The radiation energy in the maximum of the PXR reflection is $E_{PXR}^{\pi-\gamma_{eff}^{-1}} = \dfrac{c\hbar g_3}{2\sqrt{\varepsilon_0}}$. As the radiation propagates through the bent crystal it will reach the region, where it will be diffracted by the crystallographic planes $(0\bar{4}0),(0\bar{8}0),(0\,\bar{12}\,0)$ (they are parallel to the ones denoted by the reciprocal lattice vector $\vec{g}_2$) toward of cylinder axis, as the Bragg condition will be fulfilled. The angular distance between the regions, where the PXR is emitted and then diffracted, is about $\dfrac{\gamma_{eff}^{-2}}{2}$. This means that the backward-going PXR from the crystallographic planes $(4\bar{4}0),(8\bar{8}0),(12\,\bar{12}\,0)$ will be diffracted by the crystallographic planes $(0\bar{4}0),(0\bar{8}0),(0\,\bar{12}\,0)$ toward the axis f

after covering backward path of about 507, 463, 455 μm at a proton energy of 70 GeV and 69, 25, 17 μm at a proton energy of 450 GeV respectively.

Only the PXR with its polarization direction parallel to the plane of Fig. 1b will be diffracted. Thus, backward PXR polarized in the plane of Fig. 1b will be extracted and focused in the vicinity of points F_1 and F_2. The attenuation of PXR over the path in a backward direction reduces the PXR intensity. The energies are practically equal, and the shapes of angular distributions are similar to the ones of the PXR generated at the crystallographic planes (400), (800), (12 00). The maximum possible yield of backward diffracted focused PXR at the focuses was estimated with taking into account the X-ray attenuation over tangent and radial paths in the crystal and on the assumption that all backward-going PXR is diffracted.

The forward going (dynamic) PXR, as well as the synchrotron radiation and bremsstrahlung with linear polarization in the plane of Fig.2b can be diffracted by the crystallographic planes $(400),(800),(12\,00)$ to the same focuses.

RESULTS

The results of calculations for non-diffracted PXR and CXR are presented in Table 1. The X-ray radiation spectrum at points F_1 and F_2 has four spectral peaks in the 1.7 – 19.4 keV energy range, this being convenient for registration by standard X-ray spectrometric detectors. The peak at 1.74 keV is due to a non-focused non-polarized CXR, which is produced mainly by protons moving in a 13.3 μm layer at a concave side of the plate. This layer thickness is determined by X-ray attenuation in the Si crystal (see Table 1). Thus, only a little part of the total number of protons passing through the plate produces the CXR that reaches the points F_1 and F_2. The other spectral peaks are due to a focused polarized PXR. The spectral peaks of focused PXR at $E = 6.46$, 12.91, 19.37 keV are produced mainly by protons moving in the 37 μm layer at a concave side of the plate, in the 270 μm layer at the same side of the plate, and in almost the whole crystal plate thickness, respectively.

The calculated data on the backward-going diffracted focused PXR are presented in Table 2. The energy, polarization and positions of focuses are practically identical to the ones for the non-diffracted focused PXR. It be seen from Table 2 that diffracted PXR intensity is much lower than the intensity of non-diffracted PXR at a proton energy of 70 GeV. However, the intensities become comparable at a proton energy of 450 GeV, especially for high-order PXR reflections. Therefore, the yield of focused PXR in high-order reflections at high proton energies may be increased due to the contribution from the diffracted backward PXR.

The radiation sources for different spectral peaks are specifically distributed across the crystal thickness. Therefore, the measurements and analysis of relative intensities of spectral peaks may give the estimates of beam proton distribution within the thickness of the crystal. The measurements can be done for the whole crystal plate or for its separate part, provided that other parts of the plate are screened, and the X-ray detector can see only this separate part of the crystal. The CXR from the 13.3 μm layer at a convex side of the bent crystal may be registered by an X-ray detector installed opposite to the convex side of the bent crystal. The CXR intensities at both sides of the crystal should be close to each other, as the CXR is isotropic and non-focused.

The angular divergence (convergence) of focused PXR may be controlled by varying the radius of curvature R of the bent crystal. Therefore, we have an X-ray source of several centimeters in size, with a provided smooth varying of the divergence (convergence). Such a monochromatic source of polarized X-rays with a smooth variation of divergence may be useful for calibration of large-aperture X-ray equipment, for example, X-ray space telescopes [27]. The divergence (convergence) of PXR reflections from channeling particles is L/R in the plane of Fig. 1a.

The experiment on observation of focused PXR may be performed at a facility with a crystal bent for steering the proton beam having the channeling particles intensity of about or above $10^7\ p/s$. It can be seen from Table 1 that all spectral peaks have comparable intensities at a proton energy of 450 GeV, and thus, can be measured simultaneously by a spectrometric X-ray detector. The intensity of high-order spectral peaks decreases with decrease in the proton energy down to 70 GeV, but the low-index peaks still may be observed in the experiment [28].

The X-ray detector, being about 1 cm^2 square, should be installed at the point F_1 or F_2 on the axis f. The PXR from non-channeled particles can be rejected by registering X-rays in coincidence with the particles that have passed through the bent crystal in the channeling regime. There should be a vacuum connection between the bent crystal and the X-ray detector in order to observe soft X-rays, because of their attenuation in air. The X-rays of energies 1.74 and 6.46 will be absorbed practically completely over a distance of 5 m in air. However, observation of higher-energy focused PXR is possible in air. The X-rays of energies 12.91 and 19.37 keV will be attenuated by factors of about 0.23 and 0.60, respectively, within 5 m in dry air. The energies of all spectral peaks are practically independent of incident relativistic particle energy. Yet, their intensities can increase (decrease) with an increasing (decreasing) incident proton energy [14, 24].

Table 1. Properties of CXR and focused PXR induced by 70 and 450 GeV protons channeling along crystallographic planes (110) in a bent Si single-crystal plate.

Radiation		CXR Si	PXR(400)	PXR(800)	PXR(12 00)
Polarization		No	Linear	Linear	Linear
E, keV		1.74	6.46	12.91	19.37
$(\Delta E/E)_{nat}$			$3.84\cdot10^{-9}$	$1.92\cdot10^{-9}$	$1.28\cdot10^{-9}$
$(\Delta E/E)_D$			$2\cdot10^{-3}$	$2\cdot10^{-3}$	$2\cdot10^{-3}$
T_e in Si, μm		13.3	37	270	865
Protons 70 GeV	γ_{eff}^{-1}	-	$1.42\cdot10^{-2}$	$1.36\cdot10^{-2}$	$1.35\cdot10^{-2}$
	$\Delta F, mm$	-	142	136	135
	$I, \frac{quanta}{cm^2\cdot p^+}$	$1.65\cdot10^{-7}$	$9.56\cdot10^{-8}$	$1.86\cdot10^{-8}$	$1.55\cdot10^{-9}$
Protons 450 GeV	γ_{eff}^{-1}	-	$5.24\cdot10^{-3}$	$3.18\cdot10^{-3}$	$2.63\cdot10^{-3}$
	$\Delta F, mm$	-	52.4	31.8	26.3
	$I, \frac{quanta}{cm^2\cdot p^+}$	$1.94\cdot10^{-7}$	$6.90\cdot10^{-7}$	$3.32\cdot10^{-7}$	$3.98\cdot10^{-8}$

The Si single-crystal plate is 0.5 mm in thickness and $L = 5$ cm in length. The radius of crystal curvature is $R = 5$ m. The origin of radiation (CXR or focused PXR from the labled crystallographic planes) and polarization properties of the radiation are given in the first and second lines of the table, where E is the energy of spectral peaks of radiation, $(\Delta E/E)_{nat} = 1/n$ is the natural PXR spectral peak width on the axis f for a point-like detector, $(\Delta E/E)_D = b/R$ is the PXR spectral peak width for the horizontal size of the detector $b = 1$ cm, T_e is the e-fold attenuation length of radiation having the energy E in a Si single crystal, γ_{eff}^{-1} is the inverse effective relativistic factor (for comparison, the inverse relativistic factor γ^{-1} for incident 70 and 450 GeV protons is $1.34\cdot10^{-2}$ and $2.08\cdot10^{-3}$, respectively), ΔF is the distance between the points F_1 and F_2, I is the number of quanta per proton per cm^2 at the points F_1 and F_2 with X-ray attenuation in the crystal taken into account for channeling protons randomly distributed within the thickness of the plate.

Table 2. Some properties of backward-going diffracted and focused PXR induced by 70 and 450 GeV protons channeling along the crystallographic planes (110) in a bent Si single-crystal plate.

Radiation from $\vec{g}_3$	E, keV	Diffraction from $\vec{g}_2$	Protons 70 GeV $I, \frac{quanta}{cm^2\cdot p^+}$	Protons 450 GeV $I, \frac{quanta}{cm^2\cdot p^+}$
PXR $(4\bar{4}0)$	6.46	$(0\bar{4}0)$	$3.30\cdot10^{-15}$	$3.36\cdot10^{-8}$
PXR $(8\bar{8}0)$	12.91	$(0\bar{8}0)$	$3.86\cdot10^{-10}$	$3.56\cdot10^{-8}$
PXR $(12\,\overline{12}\,0)$	19.37	$(0\,\overline{12}\,0)$	$6.38\cdot10^{-11}$	$2.78\cdot10^{-8}$

The Si single-crystal plate is 0.5 mm in thickness and $L = 5$ cm in length. The radius of crystal curvature is 5 m. The origin of backward radiation (PXR from the crystallographic plane) is given in the first column of the table, E is the energy of spectral peaks of radiation, the backward-going PXR is diffracted in the crystallographic planes shown in the third column. I is the estimated maximum number of quanta per proton per cm^2 at the points F_1 and F_2 of backward-going diffracted and focused PXR. Attenuation of X-rays over backward and radial paths in the crystal is taken into account for channeling protons randomly distributed within the thickness of the plate.

DISCUSSION

Let us discuss briefly some possibilities for diffraction, extraction and focusing of other kinds of radiation emitted by relativistic particles (positrons) channeling in a long crystal. Below we will suppose that the crystal length is comparable to the dechanneling length and will discuss radiation mainly from channeling particles only.

Extraction of channeling radiation

The Bragg diffraction of channeling radiation (ChR) in one of the crystallographic planes of the same crystal, where the ChR is generated, has been considered first by Baryshevsy and Dubovskaya [35, 36, 12] and also in [37] and more recently by Nitta et al. [25,38]. The diffraction may be used for extraction of the ChR from a long crystal. The scheme of the extraction is shown in Fig. 3. Here, the ChR of frequency ω_{ChR}, equal to the Bragg frequency ω_B for the crystallographic planes denoted by the reciprocal lattice vector $\vec{g}_1$, may be extracted from a long crystal before the ChR is attenuated. The diffracted and extracted channeling radiation (DChR) is accompanied by the ordinary PXR reflection that is generated by the same relativistic particles at the crystallographic planes denoted by the reciprocal lattice vector $\vec{g}_1$. The equality of the channeling radiation frequency ω_{ChR} and the Bragg frequency ω_B may be provided by proper choice of the incident particles energy, crystal type and alignment.

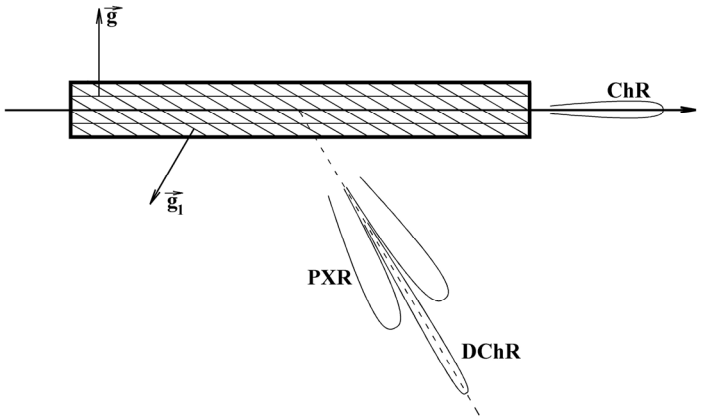

Fig.3. Extraction of channeling radiation from a perfect crystal.

Positrons or other positive particles are channeling in a perfect crystal along the crystallographic planes denoted by the reciprocal lattice vector $\vec{g}$. They emit channeling radiation (ChR) going along the particle trajectory. A part of the ChR of frequency ω_{ChR} is diffracted to the Bragg direction relative to the crystallographic planes denoted by the reciprocal lattice vector $\vec{g}_1$. The Bragg direction is shown by a dotted line. The diffraction is possible on the condition that $\omega_{ChR} = \omega_B$, where ω_B is the Bragg frequency for $\vec{g}_1$. The angular distribution of ordinary PXR reflection of frequency close to ω_B is shown schematically around the Bragg direction. The angular distribution of diffracted and extracted DChR of frequency ω_B is shown along the Bragg direction.

Focusing of channeling radiation

The channeling radiation, shown in Fig. 3, may be focused if the crystal is smoothly bent. As an example, Fig. 4 shows the focusing of ChR extracted at a right angle from a cylindrically bent crystal. Positrons are channeling along the crystallographic planes denoted by the reciprocal lattice vector $\vec{g}$. A part of channeling radiation with the frequency ω_{ChR} equal to the Bragg frequency ω_B and with the polarization in the plane of Fig. 4b is diffracted in the crystallographic planes denoted by the reciprocal lattice vector $\vec{g}_1$ and focused at point F_3 on the axis of the crystal curvature f. Besides, the tail of ChR having the frequency somewhat below ω_B can appear on the left of the axis f in Fig. 3a because of ChR diffraction at some distance from the particle trajectory. The ordinary PXR is focused at points F_1 and F_2, in much the same way as in Fig. 1. Note that the particle channeling in a bent crystal is pressed to outer wall of the channel by the centrifugal force that increases at reduction or the curvature radius. This leads to asymmetry conditions of the particle transverse motion. Evidently, that radiation of the particle in a bent crystal have to be studied itself in more details both theoretically and experimentally.

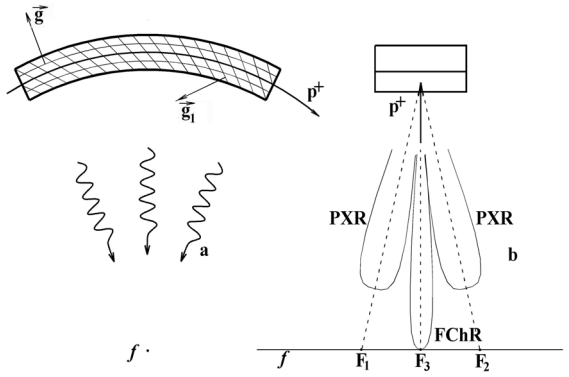

Fig. 4. Focusing of channeling radiation.
Positrons or other positive particles are channeling along the bent crystal in the crystallographic planes denoted by the reciprocal lattice vector $\vec{g}$. They emit channeling radiation of frequency $\omega_{ChR} = \omega_B$ along of particles trajectory (ω_B is the Bragg frequency relative to the crystallographic planes at 45° to the particle trajectory, that are denoted by the reciprocal lattice vector $\vec{g}_1$). The diffracted and extracted part of the channeling radiation (FChR) is focused at point F_3 . The ordinary PXR reflection is focused at points F_1 and F_2 just as in Fig. 1.

The PXR from a crystal undulator

The crystalline undulator has been proposed in [39,40]. In recent years, significant efforts have been in progress to observe the crystal undulator radiation (see, e.g. [29-31] and references therein). In experiments, relativistic particles have to move in the channeling regime along a periodically bent crystal and emit undulator radiation in the forward direction, as is shown in Fig. 5. We would like to draw attention to the fact that besides of the crystal undulator radiation (CUR), the particles should emit a number of PXR reflections in the vicinity of the Bragg directions of different crystallographic planes of the same crystal. The PXR should be rather intense, as it is generated in a long crystal. The observation of the PXR and characteristic X-rays at a significant observation angle may be useful for exact alignment of the crystal undulator and for diagnostics in the experiment. The PXR train should be frequency and phase modulated because of the periodical modulation of a crystal lattice orientation in the undulator.

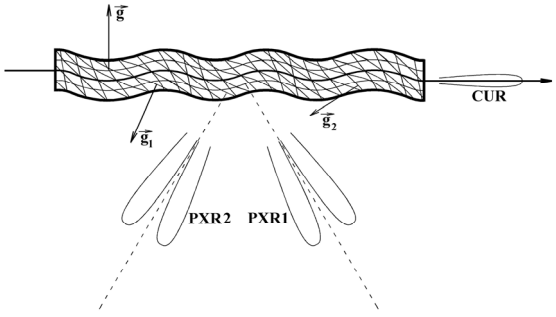

Fig. 5. Generation of PXR reflections from the crystal undulator
Positrons or other positive particles are channeling in a perfect crystal along the crystallographic planes denoted by the reciprocal lattice vector $\vec{g}$. The channeling particle emits crystal undulator radiation (CUR) in the forward direction. Besides, it emits PXR reflections in Bragg directions relative to different crystallographic planes of the crystal undulator. Only two sets of crystallographic planes denoted by the reciprocal lattice vectors $\vec{g}_1$ and $\vec{g}_2$ as well as the related Bragg directions and PXR reflections are shown in the figure.

Diffraction and extraction of crystal undulator radiation

It is obvious from Fig. 5 that the crystal undulator radiation is going through the long crystal and may be attenuated significantly. Therefore it would be of interest to extract the CUR through the side of the undulator. This may be done provided that the CUR frequency is equal to the Bragg frequency for one of the crystallographic planes, $\omega_{CUR} = \omega_B$, where ω_B is the Bragg frequency. In this case, the CUR will be diffracted and extracted from the undulator in Bragg direction similarly to the case of channeling radiation shown in Fig. 3. The exact tuning of CUR frequency may be provided by a correct choice of the incident particle energy. The angular positions of the PXR reflection, and of diffracted and extracted crystal undulator radiation (DCUR) are shown in Fig. 6. Note that the frequency band of extracted CUR may be proportional to the amplitude of the periodical crystal bend, as the Bragg condition should vary periodically, according to the crystal lattice curvature. The equality of the undulator radiation frequency ω_{CUR} and the Bragg frequency ω_B may be provided by proper choice of the incident particles energy, crystalline undulator period, the type and alignment of the crystal.

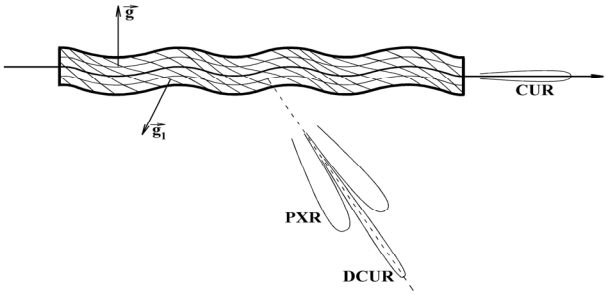

Fig. 6. Extraction of undulator radiation from the crystal undulator.

Positrons or other positive particles are channeling in a perfect crystal along the crystallographic planes denoted by the reciprocal lattice vector $\vec{g}$. The diffracted and extracted crystal undulator radiation (DCUR) is going in the Bragg direction, and the PXR reflection is around the Bragg direction for the crystallographic planes denoted by the reciprocal lattice vector $\vec{g}_1$. The frequency of CUR ω_{CUR} should satisfy to Bragg condition for these crystallographic planes, $\omega_{CUR} = \omega_B$.

Focusing of crystal undulator radiation

In some cases, the extracted CUR may be focused similarly to the above-described focusing of channeling radiation. The focusing of extracted CUR is possible from a smoothly bent crystal undulator. To exemplify, Fig. 7 shows the focusing of CUR extracted at a right angle from a cylindrically bent crystal undulator. Positrons are channeling along the crystallographic planes denoted by the reciprocal lattice vector $\vec{g}$. A part of the CUR with frequency ω_{CUR} equal to the Bragg frequency ω_B, $\omega_{CUR} = \omega_B$, is diffracted in the crystallographic planes denoted by the reciprocal lattice vector $\vec{g}_1$ and is focused at the point F_3 on the axis f of the crystal curvature. Besides, the CUR tail of frequency somewhat below ω_B may appear on the left of the axis f in Fig. 7a due to diffraction of CUR at some distance from the particle trajectory. The ordinary PXR is focused at points F_1 and F_2, just as in Fig. 1. The focused PXR train will possess the periodical frequency and phase modulation with the period $T = l/V$, where l the crystal undulator period and V is the particle velocity.

About polarization and focusing of ChR and CUR

Note that the focusing by the schemes shown in Figs. 4, 7 is optimal for focusing of radiation polarized in the plane of Figs. 4b, 7b because the reflectivity at Bragg angle $\pi/4$ is high for X-rays polarized perpendicularly to the diffraction plane and low for X-rays polarized in the diffraction plane. However ChR and CUR should be polarized mainly in the plane of Fig. 4a and 7a that is parallel to the diffraction plane. Thus, coplanar schemes shown in Figs. 4, 7 only illustrate the idea but they are not optimal for focusing of ChR and CUR. The focusing for radiation with polarization parallel to the curvature plane in Figs. 4a, 7a may be provided if we will choice another alignment of the set of crystallographic planes denoted by the reciprocal lattice vector $\vec{g}_1$. In this case the diffraction plane can be aligned at arbitrary angle to the radiation linear polarization plane. Such scheme will be described in our next publication.

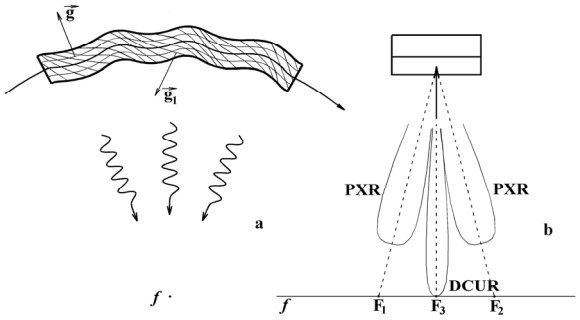

Fig. 7. Diffraction, extraction and focusing of crystal undulator radiation.
Positrons or other positive particles are channeling along a cylindrically bent crystal undulator in the crystallographic planes denoted by the reciprocal lattice vector $\vec{g}$. They emit the CUR of frequency $\omega_{CUR} = \omega_B$ along of particles trajectory (ω_B is the Bragg frequency relative to the crystallographic planes at 45° to the particle trajectory, that are denoted by the reciprocal lattice vector $\vec{g}_1$). The diffracted and extracted part of the crystal undulator radiation (DCUR) is focused at the point F_3 at axis f. The ordinary PXR reflection is focused at points F_1 and F_2 just as in Fig. 1.

CONCLUSION

In the present work we proposed several ideas and considered in short possibilities for diffraction, extraction and focusing of different kinds of radiation of relativistic particle in bent crystal. In particular, we

i. proposed the scheme for focusing of diffracted PXR, estimated main properties of diffracted focused PXR and compared them to properties of non-diffracted focused PXR described in [28].

ii. proposed the scheme for focusing of channeling radiation in bent crystal.

iii. proposed schemes for diffraction, extraction, and focusing of undulator radiation emitted from smoothly bent crystalline undulator.

We propose application of both focused PXR and CXR for online control of the bent crystal state, particle beam state and bent crystal alignment. Spectrometric X-ray detector(s) can be installed in the vicinity of the crystal curvature axis to measure X-ray spectra at one of existing stations for steering of the proton beam. The system with bent crystal and X-ray detector(s) may be planned for installation at developing facilities with proton beam energy several GeV or more. X-ray spectra can provide information for diagnostics of a part (or whole) crystal state, including its alignment, shape and degradation of crystalline structure due to radiation damages. Absolute and relative intensities of CXR and PXR spectral peaks as well as other spectral information can be rather useful for control and diagnostics of bent crystal and particle beam.

The PXR from non-channeling particle moving rectilinearly through bent crystal have to be focused at distance $R/2$ from concave side of the bent crystal and the yield of this PXR should exceed one from channeling particles described in the beginning of the paper. The focusing of PXR from non-channeling particles will be considered in more details in our next paper. Here we only note that simultaneous observation of focused PXR from channeling (at distance R from bent crystal) and focused PXR from non-channeling particles (at distance $R/2$ from crystal) would allow diagnostics of the particle beam fractions behavior in bent crystal.

Focused PXR may be rather interesting as a unique source of focused coherent X-rays with huge coherent length $l_{coh} = cL/V$ equal to wave-train length that practically is equal to the crystal length L. The value of the coherent length may be several centimeters. The wave train can be modulated by variation of the crystal structure properties along the crystal. For example, the PXR wave-train from crystalline undulator have to be modulated due to undulator periodicity.

Also, we propose to plan installation of X-ray detector(s) in the vicinity of Bragg direction(s) of crystalline undulator in forthcoming experimental research of crystal undulator radiation. Such detector(s) would allow control of the crystal undulator state and alignment and monitoring of measurements due to observation of PXR and characteristic X-ray radiation as well as observation of diffracted undulator and/or channeling radiation. The background radiation because of the bremsstrahlung in crystal undulator can be as a serious obstacle for observation and application of undulator radiation in forward direction. The spectrum of diffracted crystal undulator radiation should be free of bremsstrahlung as well as other kinds of radiation going in forward direction with different frequencies. The detector of diffracted crystal undulator radiation installed in the vicinity of the Bragg direction will not be overloaded by other kinds of radiation going in forward direction.

FINAL NOTES

The present work has been preliminary reported and discussed at NATO Advanced Research Workshop "Advanced Photon Sources and Their Application", Nor Hamberd, Armenia, August 29 – September 02, 2004 , see [32]. More recently, the diffraction, extraction and focusing of bremsstrahlung, coherent bremsstrahlung, and synchrotron radiation of relativistic particle from bent crystal have been proposed and discussed at meeting [33].

REFERENCES

1. E.N. Tsyganov Some aspects of the mechanism of a charge particle penetration through a monocrystal, Fermilab, TM-682 (1976).
2. V.M. Biryukov, Yu.A. Chesnokov, V.I. Kotov Steering of high-energy charged particle beams by bent single crystals // Uspekhi Fizicheskikh Nauk. – 1994. – V.164. – P.1017-140 [in Russian], // Physics-Uspekhi. – 1994. – V.37. – P.937-961.
3. V.A. Andreev, V.V. Baublis, E.A. Damaskinskij, A.G. Krivshich, L.G. Kudin, V.V. Marchenkov, V.F. Morozov, V.V. Neljubin, E.M. Orishchin, G.E. Petrov, G.A. Rjabov, V.M. Samsonov, L.E. Samsonov, E.M. Spiridenkov, V.V. Sulimov, O.I. Sumbaev, V.A. Schegelsky Experimental detection of the effect of volume capture in a channelling mode in the bent single crystal // Pis'ma ZhETF. – 1982. – V.36. – No 9. – P.340-343; Focussing of a beam 1 GeV protons during volume capture in a channelling mode by the bent monocrystal // Pis'ma ZhETF. – 1984. – V.39. – No 2. – P.58-61.
4. A.A. Asseev, M.Yu. Gorin Crystal-aided non-resonant extraction of 70 GeV protons from the IHEP accelerator // Nucl. Instr. and Meth. - 1996. – V. B119. – P.210-214.
5. Yu.A. Chesnokov Review of IHEP experiments for focusing and deflection 70 GeV proton beam with bent crystals // Nucl. Instr. and Meth. – 1996. – V. B119. – P.163-171.
6. K. Elsener, G. Fidecaro, M. Gyr, W. Herr, J. Klem, U. Mikkelsen, S.P. Møller, E. Uggerhøj, G. Vuagnin, E. Weisse Proton extraction from the CERN SPS using bent silicon crystals // Nucl. Instr. and Meth. – 1996. – V. B119. – P.215-230.
7. A. Baurichter, K. Kirsebom, R. Medenwaldt, S.P. Møller, T. Worm, E. Uggerhøj, C. Biino, M. Clément, N. Doble, K. Elsener, L. Gatignon, P. Grafström, U. Mikkelsen, A. Freund, Z. Vilakazi, P. Siffert, M. Hage-Ali, New results from the CERN-SPS beam deflection experiments with bent crystals // Nucl. Instr. and Meth. – 1996. – V. B119. – P.172-180.
8. N. Doble, L. Gatigton, P. Grafstrom A novel application of bent crystal channeling to the production of simultaneous particle beams // Nucl. Instr. and Meth. – 1996. – V. B119. – P.181-190.
9. C.T. Murphy, R. Carrigan, D. Chen, G. Jackson, N. Mokhov, H.-J. Shih, B. Cox, V. Golovatyuk, A. McManus, A. Bogacz, D. Cline, S. Ramachandran, J. Rhoades, J. Rosenzweig, B. Newberger, J.A. Ellison, S. Baker, C.R. Sun, W. Gabella, E. Tsyganov, A. Taratin, A. Asseev, V. Biryukov, A. Khanzadeev, T. Prokofieva, V. Samsonov, G. Solodov First results from bent crystal extraction at the Fermilab Tevatron // Nucl. Instr. and Meth. – 1996. – V. B119. – P.231-238.
10. Ya.B. Fainberg, N.A. Khizhnyak Energy losses by a charged particle passing through a laminar dielectric // Zh. Eksp. Teor. Fiz. – 1957. – V.32. – P.883-895 [in Russian].
11. M.L. Ter-Mikaelian High-Energy Electromagnetic Processes in Condensed Media, Edition of Armenian Academy of Sciences, Erevan, 1969 [in Russian]. Wiley-Interscience, New York, 1972 [in English].
12. V.G. Baryshevsky Channeling Radiation and reactions in crystals at high energies, BGU publishers, Minsk, 1982 [in Russian].
13. M.L. Ter-Mikaelian Electromagnetic radiation processes in periodic media at high energies // Uspekhi Fizicheskikh Nauk. – 2001. –V.171. – P.597-624 [in Russian]. Physics-Uspekhi. – 2001. –V.44. – P.571-596 [in English].
14. A.V. Shchagin, X.K. Maruyama Parametric X-rays, in: Accelerator-based atomic physics technique and applications, eds. S.M. Shafroth, J.C. Austin (AIP Press, New York, 1997) pp. 279-307.
15. P. Rullhusen, A. Artru, P. Dhez Novel radiation sources using relativistic electrons, World Scientific Publishers, Singapore, 1998.
16. A.V. Shchagin Investigations and properties of PXR, in: Electron-photon interactions in dense media, ed. by H. Wiedemann, NATO Science Series, II Mathematics, Physics and Chemistry, Vol. 49, Kluwer Academic Publishers, Dordrecht/Boston/London, 2002, pp. 133-151.
17. V.P. Afanasenko, V.G. Baryshevsky, R.F. Zuevsky, A.S. Lobko, A.A. Moskatelnikov, S.B. Nurushev, V.V. Panov, V.P. Potsilujko, V.V. Rykalin, S.V. Skorokhod, D.S. Shvarkov Detection of proton parametric x-ray radiation in silicon // Phys. Lett. – 1992. –V. A170. – P.315-318.
18. A.V. Shchagin Focusing of Parametric X-ray Radiation from a Bent Crystal, Communication at Workshop "Relativistic Channeling and Related Coherent Phenomena", March 23 – 26, 2004, INFL-Laboratori Nazionali di Frascati, Frascati, Italy. E-Preprint: physics/0404137 (April 2004). Correction for the preprint: Number of quanta for PXR(12 00) in Table 1 must be $3.98 \cdot 10^{-8}$ instead of $1.28 \cdot 10^{-7}$. //The Journal of Kharkiv National University, physical series "Nuclei, Particles, Fields". – 2006. – No. 721. – Issue 1/29/. – P. 45-50.
19. R.B. Fiorito, D.W. Rule, M.A. Piestrup, X.K. Maruyama, R.M. Silzer, D.M. Skopik, A.V. Shchagin Polarized angular distributions of parametric x radiation and vacuum-ultraviolet transition radiation from relativistic electrons // Phys. Rev. – 1995. – V. E51. – P.R2759-R2762.
20. A.V. Shchagin Linear polarization of parametric X-rays // Phys. Lett. – 1998. – V. A247. – P.27-36.
21. A.V. Shchagin Parametric X-rays at the right angle to the particle beam // Phys. Lett. – 1999. – V. A262. – P.383-388.
22. A.V. Shchagin, V.I. Pristupa, N.A. Khizhnyak A fine structure of parametric X-ray radiation from relativistic electrons in a crystal // Phys. Lett. –1990. –V. A148. – P.485-488.
23. K.-H. Brenzinger., B. Limburg., H. Backe., S. Dambach., H. Euteneuer., F. Hagenbuck., C. Herberg, K.H. Kaiser., O. Kettig, G. Kube, W. Lauth, H. Schope, Th. Walcher How Narrow is the Linewidth of Parametric X-Ray Radiation? // Phys. Rev. Lett. – 1997. – V. 79. – P.2462-2465.
24. A.V. Shchagin, N.A. Khizhnyak Differential properties of parametric X-ray radiation from a thin crystal // Nucl. Instr. and Meth. – 1996. – V. B119. – P.115-122.

25. T. Ikeda, Y. Matsuda, H. Nitta, Y.H. Ohtsuki Parametric X-ray radiation by relativistic channeled particles // Nucl. Instr. and Meth. – 1996. – V. B115. – P.380-383.
26. A.V. Shchagin, V.I. Pristupa, N.A. Khizhnyak K-shell ionization cross section of Si atoms by relativistic electrons // Nucl. Instr. and Meth. – 1994. – V. B84. – P.9-13.
27. A.V. Shchagin, N.A. Khizhnyak, R.B. Fiorito, D.W. Rule, X. Artru Parametric X-ray radiation for calibration of X-ray space telescopes and generation of several X-ray beams // Nucl. Instr. and Meth. – 2001. – V. B173. – P.154-159.
28. A.V. Shchagin Focusing of parametric X-ray radiation // JETP Letters. – 2004. – V. 80. – P.535-540 [in Russian].
29. S. Bellucci, S. Bini, V. M. Biryukov, Yu. A. Chesnokov, S. Dabagov, G. Giannini, V. Guidi, Yu. M. Ivanov, V. I. Kotov, V. A. Maisheev, C. Malagu, G. Martinelli, A A. Petrunin, V.V. Skorobogatov, M. Stefancich, and D. Vincenzi, Experimental Study for the Feasibility of a Crystalline Undulator // Phys. Rev. Lett. – 2003. – V. 90. – P.034801.
30. W. Krause, A.V. Korol, A.V. Solov'yov, W. Greiner Photon emission by ultra-relativistic positrons in crystalline undulator, in: Electron-photon interactions in dense media, ed. by H. Wiedemann, NATO Science Series, II Mathematics, Physics and Chemistry, Vol. 49, Kluwer Academic Publishers, Dordrecht/Boston/London, 2002, pp. 263-275.
31. R.O. Avakian, K.T. Avetyan, K.A. Ispirian, E.A. Melikyan Crystalline Micro Undulator, in: Electron-photon interactions in dense media, ed. by H. Wiedemann, NATO Science Series, II Mathematics, Physics and Chemistry, Vol. 49, Kluwer Academic Publishers, Dordrecht/Boston/London, 2002, pp. 277-282.
32. A.V. Shchagin Diffraction, extraction and focusing of parametric X-ray radiation, channeling radiation and crystal undulator radiation from a bent crystal. In: "Advanced radiation sources and applications" ed. by H. Wiedemann, NATO Science Series, II. Mathematics, Physics and Chemistry – Vol. 199, Springer, 2006, pp. 27-45. Correction of the misprint: Fig.4 in [32] should be substituted by Fig. 4 from the present paper.
33. A.V. Shchagin About focusing of parametric X-ray radiation, channeling radiation, undulator, synchrotron radiation, bremsstrahlung, coherent bremsstrahlung of the particle channeling in bent crystal. Theses of XXXVI International Conference on Physics of Interactions of Charged Particles with Crystals. Moscow, May 30 - June 1, 2006. Edition of Moscow State University, Moscow 2006, p. 84. [in Russian].
34. Yu. N. Adishchev, A. S. Artemov, S. V. Afanasiev, V. V. Boiko, M. A. Voevodin, V. I. Volkov, A. S. Gogolev, V. N. Zabaev, A. N. Efimov, Yu. V. Efremov, A. D. Kovalenko, Yu. L. Pivovarov, A. P. Potylitsyn, S. V. Romanov, Sh. Z. Saifulin, E. A. Silaev, A. M. Taratin, S. P. Timoshenkov and S. R. Uglov Detection of parametric X-ray radiation from moderately relativistic protons in crystals // JETP Letters. – 2005. - V.81. - P. 241-244.
35. V.G. Baryshevsky and I.Ya. Dubovskaya Complicated and anomalous Doppler effect for channeled positron // DAN USSR. – 1976. – V.231. – P.1335-1338. [in Russian].
36. V.G. Baryshevsky and I. Ya. Dubovskaya Angular distribution of photons from channelled particles // Journal of Phys. (C). – 1983. – V.16. – P. 3663-3672.
37. O. T. Gradovsky X-ray diffraction radiation from an oscillator in a crystal (Baryshevsky-Dubovskaya effect) // Phys. Lett. A. 1988. – V.126. – P.291-294.
38. R. Yabuki, H. Nitta, T. Ikeda, Y.H. Ohtsuki Theory of diffracted channeling radiation // Phys.Rev. B.– 2001.–V.63.– P.174112.
39. V.G. Baryshevsky, I.Ya. Dubovskaya, A.O. Grubich Generation of gamma-quanta by channeled particles in the presence of a variable external field. // Phys. Lett. A. – 1980. – V.77. – P.61-64.
40. V.V. Kaplin, S.V. Plotnikov., S.V. Vorob'ev Radiation by charged particles channeling in deformed crystals // Zh. Tech. Fiz. – 1980. – V.50. – P.1079-1081; Sov. Phys. – Tech. Phys. - 1980. – V.25. –P.650-651.

ДИФРАКЦИЯ, ЭКСТРАКЦИЯ И ФОКУСИРОВКА ПАРАМЕТРИЧЕСКОГО РЕНТГЕНОВСКОГО ИЗЛУЧЕНИЯ, ИЗЛУЧЕНИЯ ПРИ КАНАЛИРОВАНИИ И ОНДУЛЯТОРНОГО ИЗЛУЧЕНИЯ

А.В. Щагин
Национальный научный центр Харьковский Физико-Технический Институт, Харьков 61108, Украина
E-mail: shchagin@kipt.kharkov.ua

В работе описана возможность фокусировки параметрического рентгеновского излучения (ПРИ) без применения какой-либо специальной рентгеновской оптики. ПРИ испускается релятивистской заряженной частицей, движущейся в режиме каналирования вдоль изогнутого кристалла. Фокусируется ПРИ, испускаемое со всей длины изогнутого кристалла. Оценены некоторые свойства сфокусированного ПРИ и обсуждаются его возможные применения. Кроме того, описана возможность дифракции ПРИ, испущенного релятивистской частицей в изогнутом кристалле. ПРИ, испущенное от одной системы кристаллографических плоскостей, может подвергаться дифракции на другой системе кристаллографических плоскостей. Описан пример, где ПРИ испускается в направлении назад и подвергается дифракции под прямым углом. После дифракции излучение покидает тонкий кристалл и фокусируется. Оценены некоторые свойства дифрагированного сфокусированного ПРИ. Предложен эксперимент по наблюдению фокусировки ПРИ и дифрагированного ПРИ. Предложено применение сфокусированного ПРИ для оперативного контроля состояния и ориентации изогнутого кристалла и пучка. Кроме того, впервые показаны возможности дифракции, экстракции и фокусировки ондуляторного излучения из кристаллического ондулятора, а также фокусировки излучения при каналировании. Предлагается планировать установку детектора(ов) рентгеновского излучения вблизи направления(й) Брэгга в будущих экспериментах с кристаллическим ондулятором для наблюдения ондуляторного излучения и оперативного контроля состояния пучка, ондулятора и его ориентации.

КЛЮЧЕВЫЕ СЛОВА: параметрическое рентгеновское излучение, излучение при каналировании, дифракция рентгеновского излучения, изогнутый кристалл, фокусировка, мнимые изображения, фокусировка излучения при каналировании, фокусировка ондуляторного излучения.